Inorganic Chemistry, Vol. 15, No. 2, 1976 **265**

Contribution from the Department of Chemistry,
University of Glasgow, Glasgow G12 8QQ, Scotland

Single-Crystal Polarized Infrared and Raman Spectra and Normal-Coordinate Analysis of Some Group 4 Complex Hexafluorometalates

IAN W. FORREST and ANDREW P. LANE*[1]

Received June 19, 1975 AIC50435P

A normal-coordinate analysis of K_2TiF_6, Rb_2ZrF_6, and Cs_2HfF_6 was undertaken in order to assess the applicability of the Urey–Bradley potential function to ionic systems containing distorted octahedra. The calculated frequencies of the octahedral modes for the zirconium and hafnium complexes were in good agreement with those obtained from the single-crystal polarized infrared reflectance and Raman spectra of these complexes; for K_2TiF_6 the agreement was poor, the results suggesting a different TiF_6^{2-} geometry from that previously reported. Attempts to reproduce the lattice mode frequencies were less successful reflecting either the inadequacy of the potential function used or a slight error in the published cation coordinates. Interpretation of the results was facilitated by establishing the direction in which the triply degenerate modes of an MF_6 molecule split upon octahedral distortion. This was achieved by a normal-coordinate analysis of PtF_6 and WF_6 which had been artificially distorted by both elongation and flattening of the octahedron.

Introduction

Apart from K_2ZrF_6 and K_2HfF_6,[2] complex hexafluorometalates of general formula A_2MF_6 (A = NH_4, K, Rb, Cs, Tl; M = Ti, Zr, Hf) are isostructural with the trigonal form of K_2GeF_6[3] and have the space group D_{3d}^3 ($P\bar{3}m1$) with one molecule per unit cell.[4-6] In these complexes the transition metal atom is surrounded by six fluorine ions in the form of a distorted octahedron with the countercations, A, situated on a C_3 axis above and below triangular faces of the octahedron. In the Zr and Hf complexes the octahedra are compressed along this C_3 axis while in K_2TiF_6 there is reported to be slight elongation; both forms of distortion reduce the symmetry of the isolated MF_6^{2-} ion to D_{3d}.

Previous ir and Raman studies of these complexes[7-11] have resulted in nearly all of the bands, predicted from group theoretical considerations, being observed. However, since the vibrational data were obtained from powdered solids, accurate symmetry assignments could not be made.

Although force constant calculations for these trigonal complexes have so far been limited to a priori calculations of the ν_6 frequency for Cs_2TiF_6, Rb_2TiF_6,[11] and K_2GeF_6,[12] there has been considerable work done on the application of various force fields to octahedral MF_6 molecules[13-15] and complexes containing octahedral MX_6^{n-} ions.[16-18] The Urey–Bradley force field (UBFF) has been most widely used in the normal-coordinate analysis of complexes containing MX_6^{n-} octahedra and while more restricted than other force fields it has produced meaningful results especially when prior knowledge of the symmetry species of the observed vibrational bands was available.[19] The trigonal A_2MF_6 complexes provide a relatively simple system in which the effects of both crystalline environment and octahedral ion distortion can be studied. If the observed vibrational data could be reproduced by perturbation of a reasonable starting UBFF (i.e., reasonable in light of earlier work) together with the inclusion of relevant lattice interactions, then this would provide further useful evidence as to the applicability of the UBFF to octahedral systems.

Accordingly, we have recorded the polarized infrared and Raman spectra of those complexes for which suitable single crystals could be obtained, namely, K_2TiF_6, Rb_2ZrF_6, and Cs_2HfF_6. The observed bands are unambiguously assigned to their respective symmetry species and a complete normal-coordinate analysis of the Bravais unit cell of these A_2MF_6 complexes is presented.

Experimental Section

Crystals of the A_2MF_6 complexes studied were prepared by slow evaporation of saturated 40% hydrofluoric acid solutions (in platinum crucibles) containing stoichiometric quantities of the appropriate alkali metal fluoride and the transition metal dioxide. In general, the crystals grew as thin hexagonal platelets perpendicular to the c_0 axis, but for Rb_2ZrF_6 and Cs_2HfF_6 rodlike prisms were also obtained which exhibited {$\bar{1}$010} and {0001} faces of reasonable size and these were more suitable for single-crystal vibrational studies. In all cases the crystals obtained were of poor optical quality.

Infrared spectra from 10 to 400 cm^{-1} were recorded, at a resolution of 2.5 cm^{-1} on a Beckman-RIIC FS720 using an FTC 100 computer. For single-crystal reflection studies the angle of incidence was 12° and polarization of the incident radiation to better than 98% was obtained using an AIM wire grid polarizer. For K_2TiF_6, spectra of the powdered solid were recorded by compressing about 15 mg of the complex dispersed in 300 mg of powdered polyethylene into a 1-in. diameter disk. The instrument was calibrated against atmospheric water vapor. Above 400 cm^{-1} spectra were recorded at a resolution of 3 cm^{-1} on a Perkin-Elmer 237 fitted with a gold-wire grid polarizer in the common beam. Single-crystal reflectance spectra were obtained using a Wilks specular reflectance attachment with an angle of incidence of 15° and the powder spectrum of K_2TiF_6 was recorded as a KBr disk.

Polarized Raman spectra were recorded using a 90° scattering geometry on a Spex Ramalog 4 spectrophotometer at a resolution of 2 cm^{-1}. The instrument was calibrated to ±1 cm^{-1} using the plasma lines of an argon laser. The 488.0-nm line of a Coherent Radiation 52G argon laser was used as the exciting source.

Force constant calculations were performed on an IBM 370/155 computer.

Table I. Correlation Diagram for MF_6^{2-} Ions in A_2MF_6 Complexes with the D_{3d}^3 Space Group

Free-ion symmetry, O_h	Site and factor group symmetry, D_{3d}
ν_1 $A_{1g}{}^a$	$A_{1g}{}^a$
ν_2 $E_g{}^a$	$E_g{}^a$
ν_3 $T_{1u}{}^b$	$A_{2u}{}^b$
	$E_u{}^b$
ν_4 $T_{1u}{}^b$	$A_{2u}{}^b$
	$E_u{}^b$
ν_5 $T_{2g}{}^a$	$A_{1g}{}^a$
	$E_g{}^a$
ν_6 $T_{2u}{}^c$	$A_{1u}{}^c$
	$E_u{}^b$

[a] Raman active. [b] Infrared active. [c] Inactive.

Results

In Table I is given a correlation diagram for the octahedral modes in these A_2MF_6 complexes which shows that only static crystal field effects are observed since the site group of the M atom, D_{3d}, is identical with the factor group. Each triply degenerate octahedral mode is split into E and A components and ν_6, inactive under O_h selection rules, becomes ir active as a result of the reduction in symmetry to D_{3d}. In addition to

Table II. Factor Group Analysis of A_2MF_6 Complexes with Space Group $D_{3d}{}^3$ [a]

D_{3d}	N_i	T	T'	R	N'_i	Activity
A_{1g}	3		1		2	$x^2+y^2; z^2$
A_{2g}	1			1		
E_g	4		1	1	2	$x^2-y^2, xy; yz, zx$
A_{1u}	1				1	
A_{2u}	4	1	1		2	z
E_u	5	1	1		3	xy

[a] N_i = total number of modes; T = number of acoustic modes; T' = number of translatory lattice modes; R = number of rotatory lattice modes; N'_i = number of internal modes.

Table III. Observed and Calculated Frequencies (cm^{-1}) for the A_2MF_6 Complexes[a]

K_2TiF_6		Rb_2ZrF_6		Cs_2HfF_6		Symmetry assignment	O_h mode
Obsd	Calcd	Obsd	Calcd	Obsd	Calcd		
85	109	73	73	58	62	A_{1g}	TL
82	85	74	66	69	57	E_g	TL
138	117	90	94	83	86	E_g	RL
122	135	92	98	87	71	A_{2u}	TL
136	131	98	86	87	82	E_u	TL
n.o.	193	n.o.	141	n.o.	122	E_u	ν_6
281	293	192	203	184	195	A_{2u}	ν_4
315	328	240	236	217	210	E_u	
300	292	244	250	247	249	E_g	ν_5
308	325	258	267	257	258	A_{1g}	
n.o.	440	n.o.	416	n.o.	389	E_g	ν_2
600	600	522	518	490	495	A_{2u}	ν_3
615	613	537	541	498	496	E_u	
618	626	589	585	572	583	A_{1g}	ν_1

[a] n.o. = not observed; TL = translatory lattice mode; RL = rotatory lattice mode.

these internal modes of vibration, five optically active modes given by the representation

$$\Gamma_{\text{lattice}} = A_{2u} + E_u + A_{1g} + 2\,E_g$$

are predicted: four are translatory lattice modes and one, of E_g symmetry, is a rotatory lattice mode. The number and symmetry species of these lattice modes were derived from a factor group analysis[20] based upon the proposed space group and is presented in Table II. From this it can be seen that considering both internal and lattice modes, a total of seven bands should be observed in the infrared and seven in the Raman spectra of these A_2MF_6 complexes.

With the exception of K_2TiF_6, polarized infrared reflection spectra of these complexes were recorded for the ordinary and extraordinary ray giving rise to unambiguous assignments of the E_u and A_{2u} modes, respectively. The crystals of K_2TiF_6 grew as thin hexagonal plates perpendicular to the unique c_0 axis with the result that only the ordinary-ray spectrum could be recorded. The A_{2u} modes in the titanium complex were assigned by comparing the powder and ordinary-ray reflectance spectra. In all three complexes the crystals used for the infrared studies were small and of poor quality which precluded analysis of the reflectivity data by conventional methods. However, the reflectance bands were reasonably sharp and sufficiently well separated from each other so that anomalous dispersion effects, which in compounds such as $CsMnF_3$[21] and quartz[22] cause inversion of strong reflectance bands, could be ruled out. Therefore, using an established approximation when interpreting infrared reflection data,[23] vibrational frequencies were taken at the point of maximum slope on the low-frequency side of the reflectance band (with the exception of the A_{2u} modes for K_2TiF_6 which were obtained from powder data). These frequencies together with those obtained by recording the single-crystal polarized Raman spectra, the symmetry assignments of the crystal modes, and corresponding free ion modes for the three complexes are given in Table III.

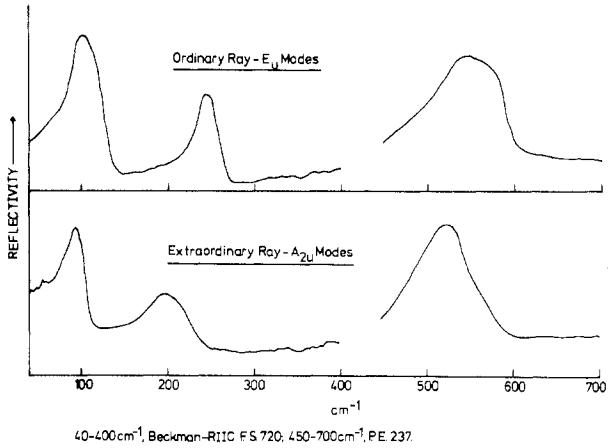

Figure 1. Polarized infrared reflectance spectra of Rb_2ZrF_6.

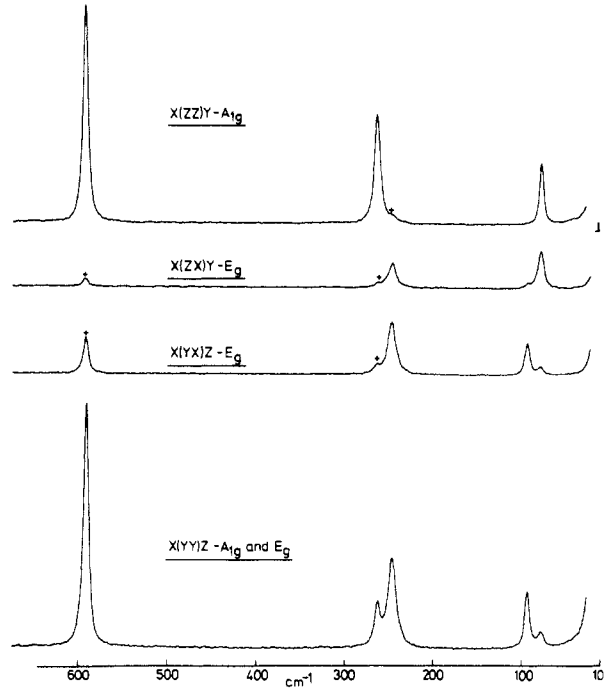

Figure 2. Polarized Raman spectra of Rb_2ZrF_6 (+ indicates polarization leakage).

Apart from frequency differences the spectral features of all of the complexes were almost identical, and in Figures 1 and 2 are presented, respectively, the polarized infrared reflectance and Raman spectra of Rb_2ZrF_6; the method of indicating the geometry used to obtain scattering from individual tensor components is that of Damen, Porto, and Tell.[24]

While group theory shows that on reducing the symmetry to D_{3d} the triply degenerate modes of an octahedron will split into a doubly degenerate and nondegenerate mode, it *does not* predict the magnitude or direction of this splitting. In order to estimate what this might be and also to assist in the normal-coordinate analysis of the A_2MF_6 complexes, several calculations were made on some MF_6 molecules using the following procedures. First, the results of a normal-coordinate analysis[14] using a UBFF were reproduced for WF_6 and PtF_6 representing, as they do, the two extremes in terms of nonbonding "d" electrons. Then, without changing the values of the force constants used in the potential function and maintaining all of the M–F bond lengths at 1.8 Å, the geometry of the MF_6 octahedron was distorted by altering the size of the FMF bond angles from 90°. The magnitude of this distortion is measured as the difference between the new FMF bond angle and 90° with the negative and positive signs in-

Table IV. Effects of Trigonal Distortion of the Frequencies (cm^{-1}) of the A and E Components of the Triply Degenerate Octahedral Modes for PtF_6 and WF_6

Distortion			Molecular symmetry			Distortion		
−12°	−7°	−2°	D_{3d}	O_h	D_{3d}	+3.5°	+6.5°	+9.5°
				a. PtF_6				
171	183	192	E_u	F_{2u} (ν_6) 195	A_{1u}	188	182	176
225	208	200	A_{1u}		E_u	198	198	198
208	227	234	A_{2u}	F_{1u} (ν_4) 238	E_u	236	235	236
256	248	241	E_u		A_{2u}	245	249	253
238	256	271	A_{1g}	F_{2g} (ν_5) 276	E_g	273	269	266
293	286	279	E_g		A_{1g}	284	290	295
668	675	683	A_{2u}	F_{1u} (ν_3) 686	E_u	684	681	679
696	692	688	E_u		A_{2u}	692	696	702
				b. WF_6				
62	105	134	E_u	F_{2u} (ν_6) 143	A_{1u}	114	78	38
234	199	160	A_{1u}		E_u	156	163	170
241	246	256	A_{2u}	F_{1u} (ν_4) 261	E_u	256	252	249
269	267	263	E_u		A_{2u}	268	276	285
255	273	290	A_{1g}	F_{2g} (ν_5) 296	E_g	291	288	285
314	306	299	E_g		A_{1g}	304	310	316
735	736	736	A_{2u}	F_{1u} (ν_3) 736	E_u	736	736	736
736	736	736	E_u		A_{2u}	736	736	737

	Force constants, mdyn/A			
	K	*H*	*F*	*F'*
PtF_6	4.22	0.149	0.13	0.02
WF_6	3.79	−0.26	0.88	−0.13

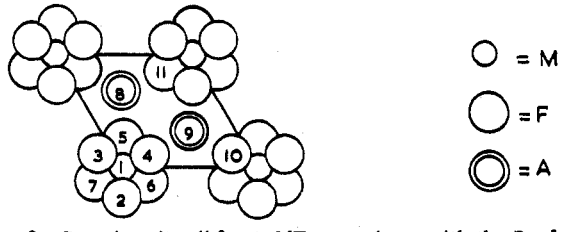

Figure 3. Bravais unit cell for A_2MF_6 complexes with the D_{3d}^3 space group. Atoms 10 and 11 are in neighboring unit cells.

dicating a flattening or elongation of the octahedron, respectively. The frequencies of the doubly degenerate and nondegenerate modes originating from the triply degenerate octahedral modes were calculated at six different FMF bond angles and the results for PtF_6 and WF_6 together with the force constants used are summarized in Table IV.

A complete normal-coordinate analysis of the A_2MF_6 complexes was performed using a Urey–Bradley potential function. In Figure 3 is shown the Bravais unit cell for an A_2MF_6 complex having the space group D_{3d}^3 together with the MF_6^{2-} octahedra in the neighboring cells which are required for a complete description of the problem. The total potential energy of the A_2MF_6 system may be considered as the sum of the potential energies associated with the isolated MF_6^{2-} octahedron and the lattice interactions as given in (1).

$$V_{total} = V_{oct} + V_{lattice} \tag{1}$$

Equation 2 gives the force field for the isolated MF_6^{2-} octahedron where the linear terms F_1', F_2', and f are related by (3).

$$2V_{oct} = K\sum_{i}^{6}(\Delta r_i)^2 + r_0^2 H\sum_{ij}^{12}(\Delta\alpha_{ij}) + F_1\sum_{ij}^{6}(\Delta R_{(1)ij})^2 + F_2\sum_{ij}^{6}(\Delta R_{(2)ij})^2 + 2R_{(1)0}F_1'\sum_{ij}^{6}(\Delta R_{(1)ij}) + 2R_{(2)0}F_2'\sum_{ij}^{6}(\Delta R_{(2)ij}) + 2r_0 f\sum_{i}^{6}(\Delta r_i) \tag{2}$$

$$f = -2(F_1' - F_2') \tag{3}$$

In constructing the equation for $V_{lattice}$ two types of lattice interactions were considered. First, there are three sets of interactions between alkali metal cations and fluorine anions but the problem was simplified by use of a common force constant k. Second, interactions between fluorine anions in neighboring molecules are taken into account; these were assumed to have quadratic and linear terms as in the case of the intramolecular fluorine–fluorine interaction. The equation for $V_{lattice}$ may thus be written as

$$2V_{lattice} = k\sum_{i}^{6}(\Delta q_1)^2 + k\sum_{i}^{6}(\Delta q_2)^2 + k\sum_{i}^{12}(\Delta q_3)^2 + F_3\sum_{ij}^{6}(\Delta R_{(3)ij})^2 + F_4\sum_{ij}^{6}(\Delta R_{(4)ij})^2 + R_{(3)0}F_3'\sum_{ij}^{6}(\Delta R_{(3)ij}) + R_{(4)0}F_4'\sum_{ij}^{6}(\Delta R_{(4)ij}) \tag{4}$$

The definition of the internal coordinates and force constants is given by reference to Table V and Figure 3.

In choosing an initial force field, trends observed in other MF_6 systems[14] were considered. Since the MF_6^{2-} octahedra do not contain any nonbonding "d" electrons, it is reasonable to assume that the "shape" of the UBFF will be similar to those of MoF_6 and WF_6. It might therefore be expected that H will be negative and the force constants F_i will have a value much larger than that based on the Lennard-Jones 6–12 potential. Furthermore, trends observed in force constant values as the position of the transition metal goes from right to left across the periodic table indicate that the stretching force constant, F, decreases, the angle bending force constant, H, increases, and the other stretching force constant, K, varies as has been shown for both MF_6 and MCl_6^{2-} molecules.[14,15]

Table V. Definition of Internal Coordinates and Force Constants

Description	Defining atoms[a]	No. of internal coordinates	Force constant (quadratic)
r	1-2	6	K
$R_{(1)}$	2-3	6	F_1
$R_{(2)}$	2-5	6	F_2
α	1-2-3	12	H
q_1	8-5	6	k_1[b]
q_2	9-3	6	k_2[b]
q_3	8-2	12	k_3[b]
$R_{(3)}$	4-10	6	F_3
$R_{(4)}$	4-11	6	F_4

[a] Atoms are numbered as given in Figure 3. [b] k_1, k_2, and k_3 are given the same value and represented by the common force constant k.

Table VI. Refined Set of Force Constants (mdyn/A) for A_2MF_6 Complexes

	K_2TiF_6	Rb_2ZrF_6	Cs_2HfF_6
K	1.88	1.70	1.41
H	−0.13	−0.16	−0.20
F_1	0.33 (2.66)	0.24 (3.09)	0.36 (3.09)
F_2	0.67 (2.74)	0.57 (2.67)	0.60 (2.72)
k	0.075	0.072	−0.085
F_3	0.21 (3.04)	0.24 (3.07)	0.21 (3.33)
F_4	0.11 (2.84)	0.10 (3.35)	0.06 (3.43)

[a] The figures in parentheses give the relevant F-F distances in angstroms.

On this basis, it was possible to choose a reasonable starting UBFF for the A_2MF_6 complexes. The angle bending force constant H was assumed to have the same value for all 12 angular coordinates and the fluorine–fluorine interaction term was taken to be dependent on the fluorine–fluorine distance. In order to simplify the problem further, the linear force constants were assumed to obey the relationship given in eq 5.

$$F_i' = -0.2F_i \tag{5}$$

The intermolecular fluorine–fluorine interaction constants were chosen in a similar fashion and the force constant k was estimated from values previously obtained for similar force constants in different systems. The force field was then refined in the usual way[17] until the best fit to the observed frequencies was obtained. The calculated frequencies for the A_2MF_6 complexes studied and the refined set of force constants are given in Tables I and VI, respectively.

Discussion

Spectra. The vibrational data obtained from the single-crystal spectra are in almost complete agreement with the group theoretical predictions except that, in all three complexes, bands corresponding to $\nu_2(E_g)$ and $\nu_6(E_u)$ were not observed. In previous infrared studies on powdered samples of these complexes[11] weak bands observed at 145 cm^{-1} in Cs_2HfF_6 and at about 170 cm^{-1} in complexes of the general formula A_2TiF_6 (A = Rb, Cs, Tl) were assigned to the ν_6 octahedral mode. Since no bands were observed in this region in the ordinary-ray reflection spectra of these complexes, despite using high-gain conditions, the earlier assignment must still be regarded as doubtful. Similarly, recording the Raman spectra of these complexes at high sensitivity failed to show any band between 300 and 500 cm^{-1} which is the region where the ν_2 mode should be observed. This is not surprising since in the Raman spectra of hexafluoride complexes such as $LiSbF_6$, Na_2SnF_6,[12] and $BaTiF_6$[26] the ν_2 mode was observed as a very weak intensity band while in the hexachloro anions $ReCl_6^{2-}$ and $OsCl_6^{2-}$ it could not be detected.[27]

Normal-Coordinate Analysis. From Table IV it can be seen that on elongation of an MF_6 octahedron, resulting in D_{3d} symmetry, the doubly degenerate E components of the ν_3, ν_4, and ν_5 modes occur at lower frequency than the nondegenerate

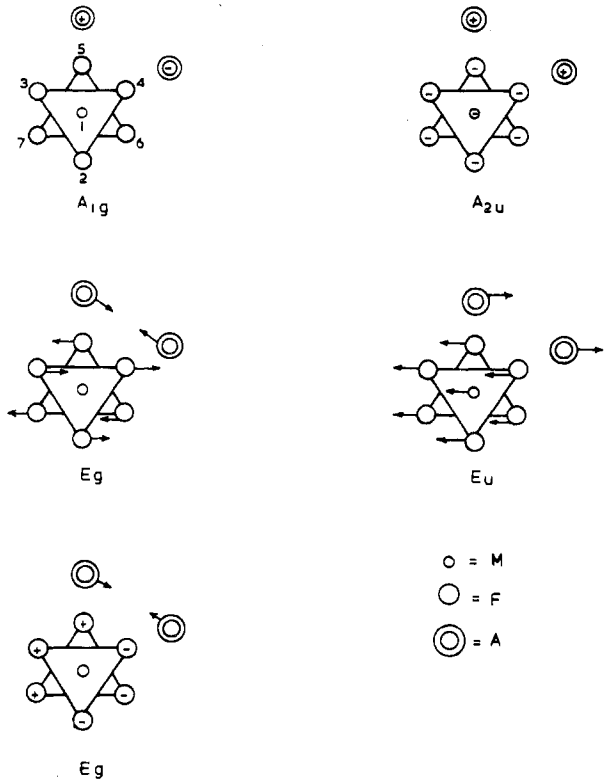

Figure 4. Normal coordinates for lattice modes in A_2MF_6 complexes with the D_{3d}^3 space group.

A component while for ν_6 the E component is at higher frequency. This situation is completely reversed for a flattened octahedron. These general conclusions apply both to PtF_6 and WF_6 although there are some differences as to the magnitude of the A–E splitting. For example, in WF_6 there is virtually no splitting of the ν_3 mode as a result of trigonal distortion whereas ν_6 shows a far greater splitting than the corresponding mode in PtF_6.

These simple calculations serve to indicate that the *direction* of splitting of the fundamental modes of an octahedron, on trigonal distortion, will differ depending upon whether the octahedron is flattened or elongated. In all the A_2MF_6 complexes studied the direction of the octahedral mode splitting was the same with the E_u species at higher frequency than the A_{2u} species for ν_3 and ν_4 and with A_{1g} higher than E_g for the ν_5 mode. While this splitting direction is not completely identical with that calculated for a flattened MF_6 octahedron, probably due to fluorine–fluorine interaction, it would suggest that, contrary to the x-ray structural data, the distortion of the MF_6^{2-} octahedra is the same for all three complexes. Further evidence to this effect was obtained from the results of the normal-coordinate analysis.

In the normal-coordinate analysis it was possible, for all three complexes, to reproduce the splitting direction of the triply degenerate modes provided the intermolecular fluorine–fluorine interactions (both linear and quadratic) were included. However the internal mode frequencies could not be reproduced using a force field similar to that for PtF_6 which contains four nonbonding d electrons. The expected inverse relationship between the fluorine–fluorine interaction constants F_i and the corresponding fluorine–fluorine distances was not found in the case of K_2TiF_6. In effect, the refinement process is artificially flattening the TiF_6^{2-} octahedron again suggesting an error in the structural data as to the detailed positioning of the fluorine ions.

The potential energy distribution and normal coordinates of the internal modes showed that there was only a small amount of mixing with the lattice modes with the result that

the normal description of the octahedral modes, as given in Table III, is reasonably accurate. The deviation from a purely distorted ion model is due to the relatively short intermolecular fluorine–fluorine distances and the consequent necessity of including fluorine–fluorine interaction terms. These A_2MF_6 complexes, therefore, do not constitute a particularly good system for studying the application of the UBFF to a distorted octahedron in isolation. However, it should be emphasized that if the experimental symmetry assignments were disregarded, then an apparent fit to the observed frequencies could have been obtained *without* the inclusion of lattice interactions. This latter point illustrates the dangers of normal-coordinate analysis of solid-state systems without prior knowledge as to the symmetry species of the observed bands.

The normal coordinates of the lattice modes are shown diagrammatically in Figure 4. The higher frequency E_g mode can be assigned to the rotatory lattice mode although there is some translational motion of the cations. The frequency of this mode cannot be reproduced without the inclusion of the fluorine–fluorine interaction term, but in K_2TiF_6 it occurs 21 cm^{-1} below the observed value. This, again, could be explained on the basis of a mistaken TiF_6^{2-} geometry. Since mixing between internal and lattice modes is minimal, the translatory lattice modes can be simply described as an out-of-phase vibration of the ions in the *xy* plane (E modes) or along the *z* axis (A modes). However the agreement between the observed and calculated frequencies for the translatory lattice modes is, in general, poor even for Rb_2ZrF_6 and Cs_2HfF_6. The E modes are observed at higher frequency than the A modes whereas they are calculated in the reverse order. Part of the explanation for this might lie in the restriction which was imposed on the cation–fluorine interaction constants, but if these are allowed to vary randomly, then refined values are obtained which are unrelated to the ion–ion distances involved. This may be another indication of a slight error in positioning of the ions in the crystal structure analysis since a change in the position of the alkali metal ion along the *z* axis could easily reverse the calculated frequencies of the E and A modes. However, by giving the three types of cation–fluorine interaction a single value, any structural inaccuracies of this type would not be apparent. Alternatively, it should be emphasized that the force field may simply be inadequate to describe lattice interactions fully although it is difficult to envisage, considering other work in this field, how any improvement could be made.

Acknowledgment. We gratefully acknowledge support of this work by the Science Research Council which provided a graduate studentship grant (to I.W.F.) and a grant toward the purchase of the laser Raman instrument. Acknowledgment is also made to the Equipment Sub-Committee of Glasgow University for partial support of this research.

Registry No. K_2TiF_6, 16919-27-0; Rb_2ZrF_6, 16962-10-0; Cs_2HfF_6, 16919-32-7; PtF_6, 13693-05-5; WF_6, 7783-82-6.

References and Notes

(1) To whom correspondence should be addressed.
(2) H. Bode and G. Teufer, *Acta Crystallogr.*, **9**, 929 (1956).
(3) J. L. Hoard and W. B. Vincent, *J. Am. Chem. Soc.*, **61**, 2849 (1939).
(4) H. Bode and G. Teufer, *Z. Anorg. Allg. Chem.*, **283**, 18 (1956).
(5) S. Siegel, *Acta Crystallogr.*, **5**, 683 (1952).
(6) B. Cox and A. G. Sharpe, *J. Chem. Soc.*, 1783 (1953).
(7) R. D. Peacock and D. W. A. Sharp, *J. Chem. Soc.*, 2762 (1959).
(8) D. H. Brown, K. R. Dixon, C. M. Livingstone, R. H. Nuttall, and D. W. A. Sharp, *J. Chem. Soc. A*, 100 (1967).
(9) P. A. W. Dean and D. F. Evans, *J. Chem. Soc. A*, 698 (1967).
(10) P. W. Smith, R. Stoissinger, and A. G. Turnbull, *J. Chem. Soc. A*, 3013 (1968).
(11) A. P. Lane and D. W. A. Sharp, *J. Chem. Soc. A*, 2942 (1969).
(12) G. M. Begun and A. C. Rutenberg, *Inorg. Chem.*, **6**, 2212 (1967).
(13) B. Weinstock and G. L. Goodman, *Adv. Chem. Phys.*, **11**, 169 (1965).
(14) H. Kim, P. A. Sonder, and H. H. Claasen, *J. Mol. Spectrosc.*, **26**, 46 (1968).
(15) P. Labonville, J. R. Ferraro, M. C. Wall, and L. J. Basile, *Coord. Chem. Rev.* **7**, 257 (1971).
(16) M. J. Reisfeld, *Coord. Chem. Rev.*, **29**, 120 (1969).
(17) J. Hiraishi, I. Nakagawa, and T. Shimanouchi, *Spectrochim. Acta*, **20**, 819 (1964).
(18) I. R. Beatie, T. R. Gibson, and G. Ozin, *J. Chem. Soc. A*, 2765 (1968).
(19) J. D. Black, J. T. R. Dunsmuir, I. W. Forrest, and A. P. Lane, *Inorg. Chem.*, **14**, 1257 (1975).
(20) D. M. Adams and D. C. Newton, "Tables for Factor Group and Point Group Analysis", Beckman-RIIC Ltd., London, 1970.
(21) J. T. R. Dunsmuir, I. W. Forrest, and A. P. Lane, *Mater. Res. Bull.*, **7**, 525 (1972).
(22) W. G. Spitzer and D. Kleinman, *Phys. Rev.*, **121**, 1324 (1961).
(23) W. G. Spitzer, D. Kleinman, and D. Walsh, *Phys. Rev.*, **113**, 127 (1959).
(24) T. C. Damen, S. P. S. Porto, and B. Tell, *Phys. Rev.*, **142**, 570 (1966).
(25) A negative value for the angle-bending force constant *H*, found for molecules having no nonbonding electrons, occurs not only when using the UBFF but also with the orbital valence force field. We agree with the comments in ref 14 that a negative value for *H* is physically meaningful indicating that the fluorine–fluorine repulsions are sufficiently strong to prevent the molecule distorting from O_h symmetry.
(26) S. P. Beaton, unpublished results.
(27) L. A. Woodward and M. J. Ware, *Spectrochim. Acta*, **20**, 711 (1964).

Contribution from the Department of Chemistry,
Rutgers University, New Brunswick, New Jersey 08903

Analysis of the Vibrational Spectra of μ-Oxo-Bridged Complexes[1]

JOSEPH SAN FILIPPO, Jr.,* ROBERT L. GRAYSON, and HENRY J. SNIADOCH

Received July 2, 1975 AIC50461N

Analysis of the Raman spectra of several representative linear μ-oxo-bridged complexes reveals that the symmetrical metal–oxygen–metal stretching vibration is significantly lower than the corresponding vibration observed in bent μ-oxo-bridged complexes. The utility of this result as it relates to the study of the μ-oxo-decahalo ions $[Ru_2OCl_{10}]^{4-}$, $[Os_2OCl_{10}]^{4-}$, $[W_2OCl_{10}]^{4-}$, and other μ-oxo-bridged complexes is discussed.

Infrared spectroscopy is well established as a technique of general usefulness in structural investigations of oxometal complexes.[2-5] These compounds frequently display characteristic absorptions in regions of the infrared spectrum that are readily accessible to general instrumentation. However, characterization of the important class of oxometal complexes which contain ir-inactive metal–oxygen vibrations and/or metal–oxygen vibrations which occur in the low-energy region of the vibrational spectrum and, consequently, cannot be investigated with routine infrared instrumentation remains a difficult problem. Although single-crystal x-ray diffraction studies are being carried out on an increasing number of complexes, development of an alternative spectroscopic approach to the study of this family of complexes would constitute a useful addition to the range of techniques applicable to the examination of these materials.

The work reported in this paper was initiated in the hope that Raman spectroscopy could be applied to the structural characterization of certain oxometal complexes. Here we wish to report the results of an investigation stressing the qualitative